

NUMERICAL MODELING OF SHALLOW LANDSLIDE IMPACTS ON FLEXIBLE PROTECTION SYSTEMS AND ITS VALIDATION WITH FULL SCALE TESTING

Albrecht v. BOETTICHER*, Axel Volkwein*, Roland Wüchner[†], Kai-Uwe
Bletzinger[†], Corinna Wendeler[#]

*Swiss Federal Institute for Forest, Snow & Landscape Research (WSL)
Zürcherstrasse 111
8903 Birmensdorf, Switzerland
e-mail: {albrecht.vonboetticher, volkwein}@wsl.ch, www.wsl.ch/fe/lms

[†]Technical University of Munich (TUM)
80290 Munich, Germany
e-mail: {wuechner, kub}@bv.tum.de, www.st.bv.tum.de

[#]Geobrugg AG - Protection Systems
Aachstrasse 11
8590 Romanshorn, Switzerland
e-mail: corinna.wendeler@geobrugg.com, www.geobrugg.com

Key words: Shallow Landslides, Coupled Problems, Freeface Flow, Natural Hazard Protection, Chain-Link Finite Element

Abstract. Innovative flexible protection barriers against shallow landslides, made from high tensile steel meshes, demanded the development of numerical models for the different mesh types accompanied with 1:1 scale prototype field testing. To generate the barrier model, a special Discrete Element had to be developed that represents the chain link type of steel mesh. It was crucial that it includes the complex out-of-plane height of the mesh that accomodates the local high deformations of the net. The filling process of the barrier is simulated using OpenFOAM, taking the fluid-structure interaction with high deformations into account. In addition to the shear thinning behaviour of the mud, the turbulence in form of a large eddy simulation can be introduced, having regard to the interaction with the complex geometry and free surface by a Dynamic Mixed Model approach for the subgrid scales. The model is validated with 1:1 scale tests where shots of 50 m³ of mud travel down a 40 m long slope and hit the barrier.

1 INTRODUCTION

Shallow landslides are natural hazards of increasing importance, making the development of protection barriers that can retain a shallow landslide impact a very important issue. Flexible protection systems against rockfall or shallow landslides have certain advantages compared to rigid protection walls. Their main advantage is the transfer of the impact energy to anchors over time, with brake elements designed to consume the impact energy through plastic deformation. This way, a flexible protection system can slowly decelerate the impact and control peak forces throughout the structure. With protection nets made out of high-tension steel wire, carried by support ropes that are lead over steel posts to ground anchors, low weight barriers were developed that can be installed without much intervention to the slope. They have the capability to catch high energy rapid mass movements like rockfall or shallow landslides. A successful design of this kind of protection systems needs to trace the dynamic behaviour of all involved parts and needs to adjust their dimensioning to the energy transfer through the system. In general, this procedure demands 1:1 scale testing so there is a high demand for numerical models that reduce the number of tests necessary to find a successful design. This work focuses on two challenging issues within this context, the numerical model for *chain-link* steel meshes, and the simulation of the dynamic interaction of a shallow landslide impact with the barrier. The aim of this work is to improve the current state of the art of shallow landslide barrier design, where the whole filling process still is replaced with a static analysis and an equally distributed force.

2 CHAIN-LINK TYPED STEEL NETS

There are a wide range of different mesh structures. The *chain-link* meshes normally found in the design of standard fence structures gain increasing use in setups using high-strength steel due to its enormous capacity to retain loads while having a low need of steel material. Figure 1 shows the general geometry of a chain link mesh and its representation as *elements*, *segments* and the mesh junctions as *nodes* for numerical discretization. The performance of the mesh is dependent on non-trivial processes in the mesh nodes that control the maximal load the mesh can take and the development of the mesh stiffness under high stress.

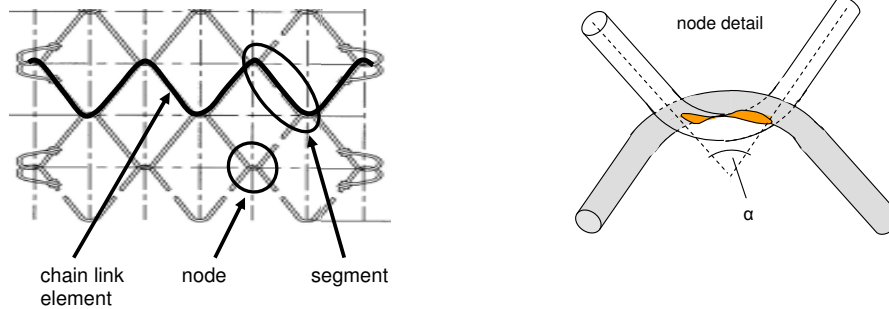


Figure 1: An *element* represents a wire (bundle), a *segment* specifies the element section from net node to net node. At the *node* (right), two elements cross each other in accordance with the mesh angle α and form a contact area between them.

2.1 Angle dependent performance

A series of quasi-static in-plane tension tests (Fig. 2) have demonstrated that the limit load of a segment depends on the mesh angle α . Net samples fixed on all borders and loaded by dragging one border can take about 30% more load when deformed in the direction of the elements than if pulled in an orthogonal direction. This is caused by the increase of the element length that leads to increasing mesh angles, while an orthogonal deformation of the sample causes increasing element widths with decreasing angles.



Figure 2: A TECCO type net is pulled in mesh direction decreasing the mesh angle while deforming.

2.2 Numerical approach of the discrete chain-link finite element

The test samples failed at the net nodes. With detailed modelling of the node geometry in dependency of the mesh angle, the combined normal force, shear and momentum of the wire along the node could be calculated. As failure criteria, the section with the highest normal force and shear interaction was defined. At this section, the steel wire resistance combining shear, normal force and bending was re-checked. With only varying

the steel material properties and the net geometry, the maximal load of plane tensile tests of different mesh types with single wire elements could be predicted with $\pm 5\%$ accuracy.

The net stiffness is not directly related to the stiffness of the steel wire but is dominated by the bending resistance of the segments at the nodes. The out-of-plane-height of the mesh construction provides reserves for locally high deformations that can develop with plastic bending deformations. Two opposite processes occur under loading, one leading to an increase of net stiffness by reducing the out-of-plane-height of the mesh and one that decreases the net stiffness by normal stress - bending interaction. By including these processes to the model, it was possible to simulate the longitudinal and transversal plane tensile tests with good accuracy, matching the maximal deformations with $\pm 6\%$.

The high computational costs needed for such a detailed approach (about three hours to simulate one second of a mesh specimen containing 200 segments on an Intel dual core machine, 3GHz) led to a simplified model that takes advantage of the nearly linear-plastic behaviour but accommodates the dependency to the mesh angle. The discrete chain-link finite element model uses instead the maximal load per mesh width, the maximal load per mesh length and the corresponding maximal deformations as input parameters. This information can be found on the mesh type data sheets and is usually generated from plane tension tests with 1 x 1 m specimen.

2.3 Calibration

The stiffness of the 1 x 1 m specimen under plane loads is not very representative for a large scale net under out-of-plane impact. Therefore, the two maximal deformation input parameters for the discrete chain-link finite element were calibrated for each net type by vertical impact tests, where a 820 kg concrete ball with accelerometers embedded in its core was dropped into a 3.5 x 3.5 m net (Fig. 3 left). The corresponding simulation (Fig. 3 right) shows the discrete chain link finite element integrated in the software FARO^[1]. A comparison of simulation to measurement data obtained with load cells installed in the steel frame, the accelerations measured in the ball and its position captured with high speed cameras (Fig. 3 middle) shows the impact of the ball, its acceleration back in the air and a second impact when the ball drops back in the net.

2.4 Validation

Full scale rockfall tests were taken as validation for the chain-link finite element. Two vertical high impact tests were used, one with a 1600 kg concrete block generating a 500 kJ rockfall impact (Fig. 4) and one with a 3200 kg concrete block and 1000 kJ of impact energy. At both tests, the block reached the net with 25 m/s velocity. The quality of the simulation was observed comparing the simulated and measured time delay of the impact, the maximal rock displacement and the rope forces. The process is reproduced with good accuracy concerning the time delay, and the maximal displacement of the rock from the moment of contact to the moment of standstill is predicted within $\pm 10\%$ difference.

The forces of ropes that are connected to brake elements show good results as in Fig. 3 (middle), overestimating the forces by maximal 13% dependent on the brake element material law. The retaining ropes holding the posts tend to develop dynamic oscillation which is a problem of the rope element. It occurs independent of the chain-link mesh and is subject to further investigation.

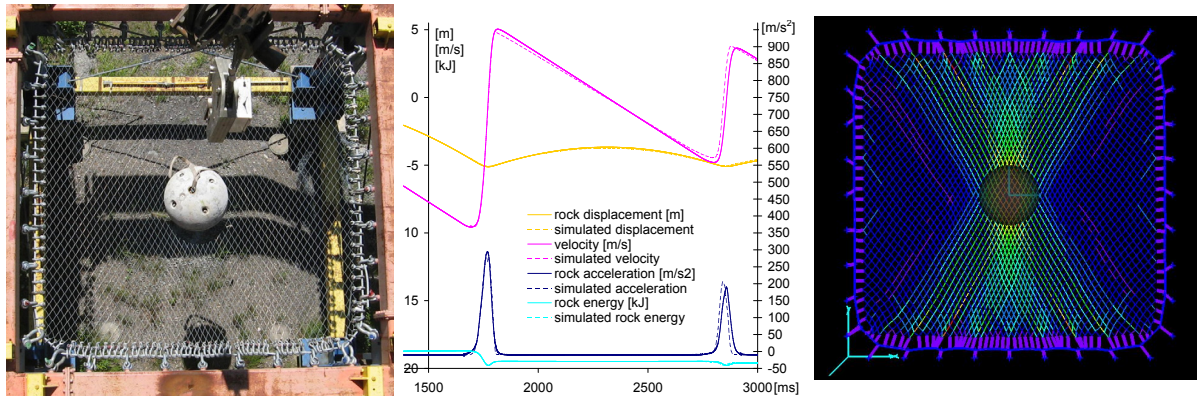


Figure 3: Test site (left), corresponding model (right) and comparison of the calibrated model with curves from experimental data over time in [ms] (middle).

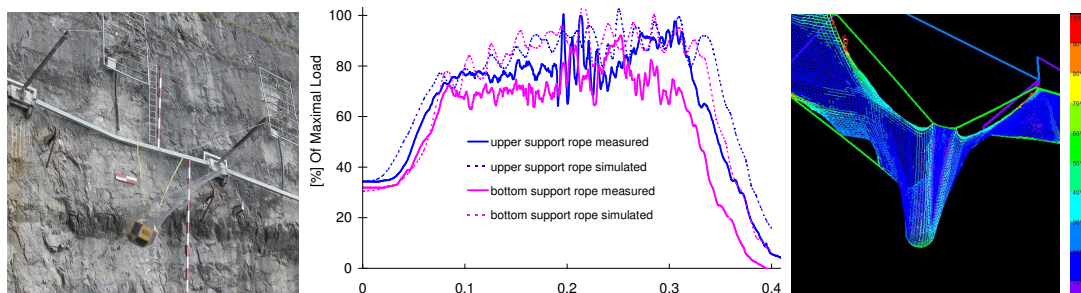


Figure 4: A 500 kg concrete block hits the barrier with 25 m/s (left), calculated and measured rope forces over time in [s] (middle) and the corresponding simulation with colours representing the degree of utilisation (right).

3 SHALLOW LANDSLIDE IMPACT WITH CFD

A crucial factor in the process of development of shallow landslide protection systems is the determination of the landslide impact pressure. Extensive research is in progress to clarify the shallow landslide dynamics and to allow the two dimensional simulation of flow head, density and mean velocity over a slope surface. Derived from depth averaged simulations with two phases, properties like density, water content, flow head and the mean front velocity can be estimated for the moment of impact at the barrier^[2]. These properties were treated as input parameters to a three-dimensional model that represents

the impact area by a finite volume grid that can handle dynamic mesh movements. Due to the local scale of the barrier impact and its short process, the shallow landslide material can be treated as homogenous. It is represented with a two phase freeface flow model processed by using the computational fluid dynamics of OpenFOAM^[3]. The *Volume of Fluid (VOF)* approach was chosen to trace the interface between air and mud, and the mud was represented as a *Herschel-Bulkley* fluid. The solver *InterDyMFoam* was chosen which can handle dynamic mesh deformations, two face flow and turbulence. The shallow landslide impacts studied in this work were dominated by laminar flow, but turbulence in high suspension flows is a focus of ongoing research^{[5][6]}. Therefore, as an option, the *Large Eddy Simulation (LES)* turbulence model of the solver accounting for complex geometry, was combined with the *Dynamic Mixed Model* for the subgrid scales that treats the surface influence and the backscatter effect in an appropriate way^[7]. The corresponding code was developed at LTT Rostock^[4].

3.1 Solver validation

As a check on the performance of the solver, three channel flow experiments with three sets of water inflow to a 2 m long and 0.3 m wide channel were carried out, and the surface velocity was measured with high-speed video tracking suberic particles^[8]. The Reynolds number reached from transient to fully turbulent flow. The simulation using the LES turbulence model, applied the Dynamic Mixed Model for the subgrid scales together with a successful clipping procedure^[9], both implemented by the LTT Rostock. The average surface flow velocity in the simulation fitted the measured results with $\pm 4\%$. Figure 5 presents the simulation grid with the freeface flow velocity.

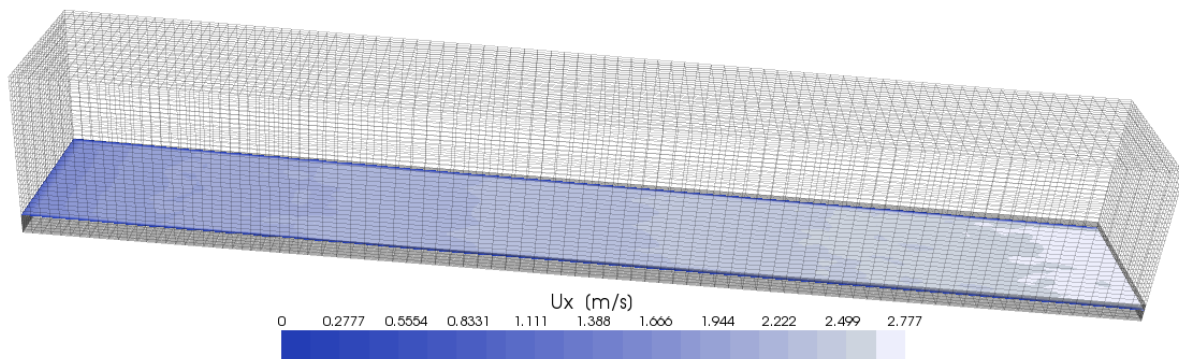


Figure 5: Simulation of a freeface channel flow, 2m long and 0.3m wide, with 20.4 l/s inflow on the left side and 5° inclination.

4 FSI COUPLING

The fluid structure interaction between the FARO structure code and the OpenFOAM CFD simulation was carried out by explicit weak coupling. After a defined interaction interval has passed, FARO sends the barrier deformation to the InterDyMFoam solver

which performs the corresponding mesh deformation to fit the front patch of the simulation grid to the barrier shape defined in FARO, and the InterDyMFoam solver sends the forces at each front cell face to FARO where they are applied to barrier nodes (Fig. 6).

4.1 Boundary condition between non-matching grids

For the development of different barrier types it is necessary to allow maximal precision in the barrier model while guaranteeing a certain independency of the CFD simulation from the geometry details of the construction. The deformation of the barrier model simulates the dynamic behaviour of the structure including the wave propagation through the non-loaded net when the front of the landslide hits the net at its bottom. Thereby, the deformation of the net has strong variations on small scales. For the OpenFOAM solver, it is necessary to avoid deformations where a cell face travels through the cells opposite face causing negative cell volumes and false cell orientations. For that reason, instead of linking the nodes of the finite volume grid boundary to the barrier nodes in a fixed manner, the interaction was implemented as a sliding interface: At every interaction step, each cell node belonging to the finite volume grid boundary searches for barrier nodes that lie momentarily closest to a slope-parallel projection of the cell nodes. Then, the boundary nodes of OpenFOAM perform a displacement along their slope parallel projection so that they get placed along the three closest barrier nodes of the FARO simulation.

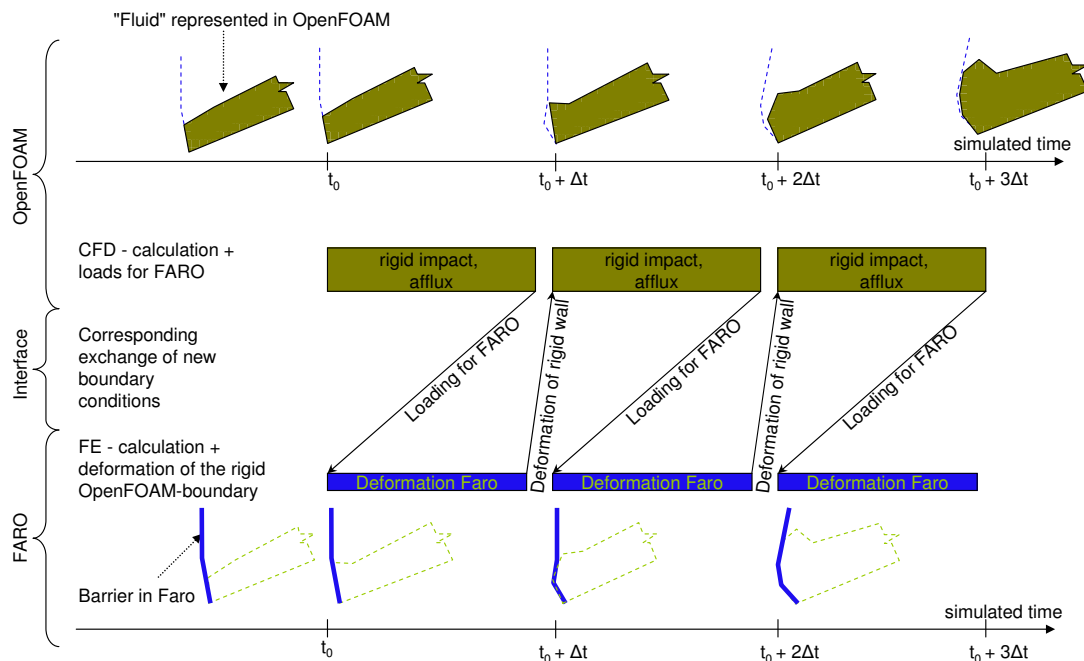


Figure 6: Fluid-structure-interaction between FARO and OpenFOAM: Stepwise update of fluid and barrier dynamics.

4.2 Modelling the area above the barrier

The barrier decelerates the impact and causes the flow to form a wave with a counter-current, which can develop higher than the top end of the barrier. It was necessary to extend the finite volume grid in such way that it reaches about one meter higher than the barrier. This fact caused a concave discontinuity at the front boundary shape. With increasing barrier deformations, cells became false orientated and caused solver instability (Fig. 7). It became necessary to smoothen the edge of the finite volume grid at the upper barrier border (upper support rope) by moving all nodes of the finite volume boundary, which are positioned higher than a cell row below the upper support rope. A successful implementation that can handle different barrier types takes the deformation at the upper support rope and multiplies it with a factor dependent to the point with the maximal barrier deformation. Then this increased upper support rope deformation is applied along all finite volume nodes positioned higher than the upper support rope region, but with an applied linear decrease with height.

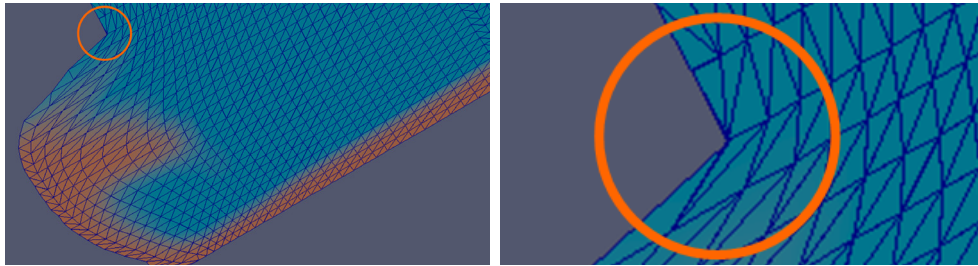


Figure 7: Cut through the simulation grid showing the two phases by colour. The circle marks the concave discontinuity of the front where the back face of the cell interpenetrates the front.

4.3 Data exchange

The exchange of forces and deformations between the OpenFOAM and FARO models is processed via input and output file streams. Initially, the interface writes a file with the position of the nodes at the boundary of the finite volume grid. The FARO code reads and stores these initial positions, and at each interaction step it calculates the discrepancy between these initial positions and their slope-parallel projection on the FARO-barrier. Then the discrepancy is written into a file as displacement vectors, one line for each OpenFoam boundary node. The InterDyMFoam solver reads in these displacement vectors and applies them to the grid over the next interaction interval with its internal dynamic mesh solver. But before starting the next interval, it calculates forces for each OpenFoam boundary node that represent the pressure at the boundary, and writes these force vectors to another file. FARO then reads these forces and distributes them: Each OpenFoam boundary node force is distributed along three FARO nodes, that lie closest to the slope parallel projection of the corresponding OpenFoam boundary node.

The timing of reading and writing, and the control of one simulation waiting for the

other to finish the current interaction interval, is done by two flags written to another two files that store the stage of each simulation. Fig. 8 shows the interface part of the flowchart with the OpenFOAM solver waiting for FARO until FARO has read the forces and written the displacements of the current interaction step. OpenFOAM then reads the displacements, calculates and writes the forces and continues the simulation. Problematic was the file sharing without lock that allows reading the number of CFD interactions while they are written. As a workaround there are currently two file stream readers following each other and comparing the tokens they read. If the tokens match, it is assumed that this token was not overwritten during reading.

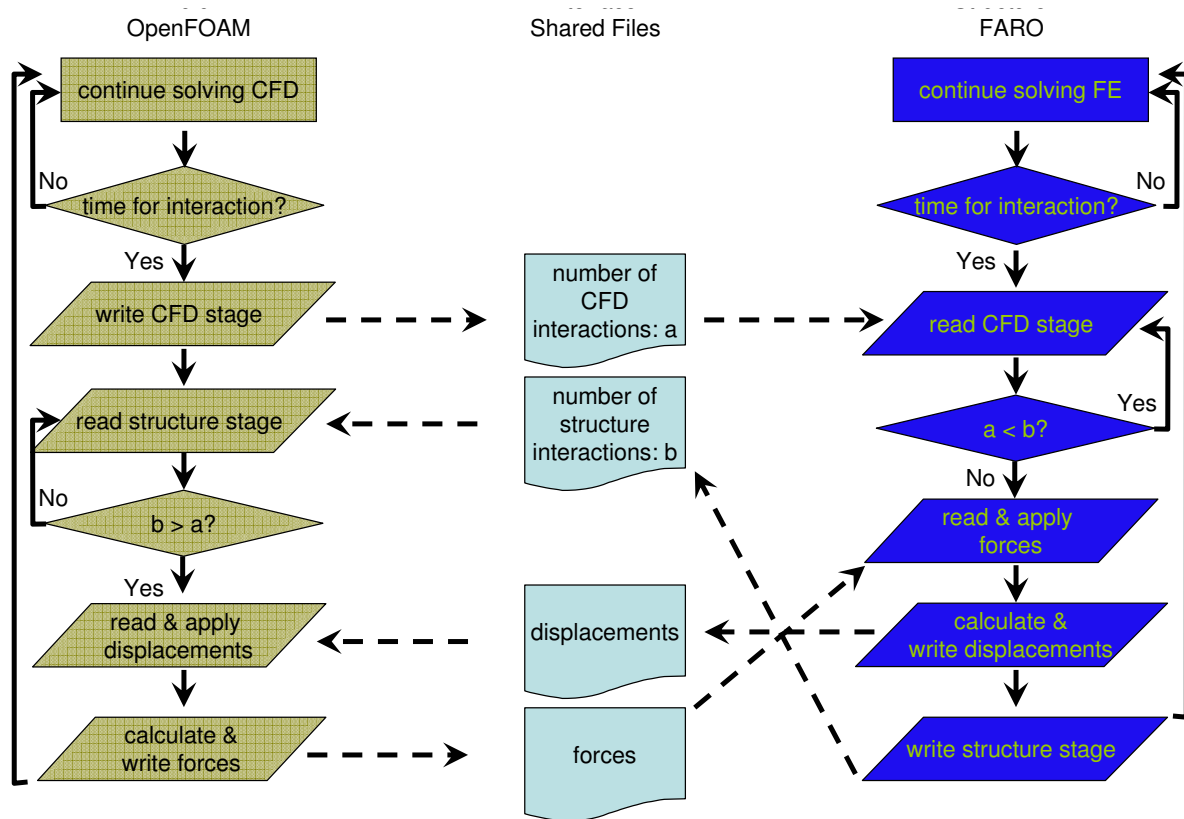


Figure 8: Part of a flowchart of the interface processes in OpenFOAM. From “write CFD stage” to “write structure stage” OpenFOAM stays in the “read structure stage” loop.

4.4 Execution time

The speed of the calculation is limited by the need for exchange between the two codes. It is not an issue of time consumption for data transfer, the files written and read at an interaction stage typically need less than 100 Kb all together. But the solver for the two phase flow could perform much higher timesteps by the use of its automatic time step control that allows speeding up the solution at stages where the flow proceeds with low

courant numbers. The need for a small interaction interval to avoid pressure oscillations limits the time step, so the simulation currently takes four hours for the simulation of one second of impact on a standard dual core PC.

4.5 Testing

A wide number of 1:1 scale test have been realized, were up to 50 cubic meters of mud travel down a 30 m long slope, passing three flow head measurement points carried out with laser, a ground plate taking the weight and tangential force of the flow and two vertical force plates that register the impact pressure. Finally the artificial shallow landslides hit the flexible barrier and activate four tension load cells installed at the support ropes and retaining ropes of the barrier^[10].

4.6 Results

First outputs of one simulated test give promising results: The impact pressures of the model lie below the ones measured by the rigid impact force plates that reached 90000 Pa, see Fig. 10. This fits the assumption that the flexible barrier results in lower pressures than a rigid wall. Upper support rope forces and retaining rope forces fit well to the measured maxima and the development over time (Fig. 9). After the impact, material slowly leaves the barrier towards the sides. That effect is overestimated leading to a faster decrease of static loads in the simulation.

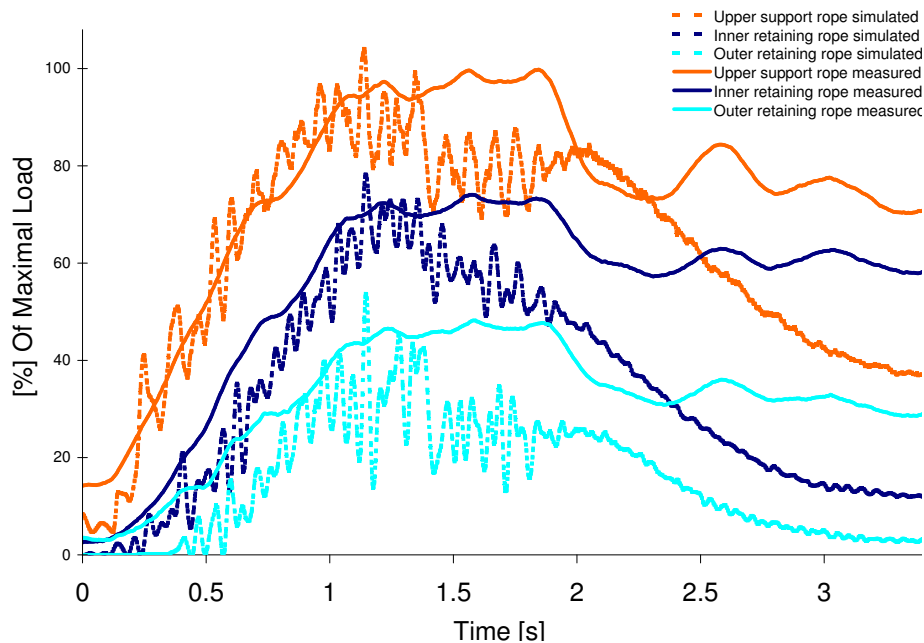


Figure 9: Measured and simulated rope forces taken from the 7th test performed at the WSL-test side in Veltheim, Switzerland.

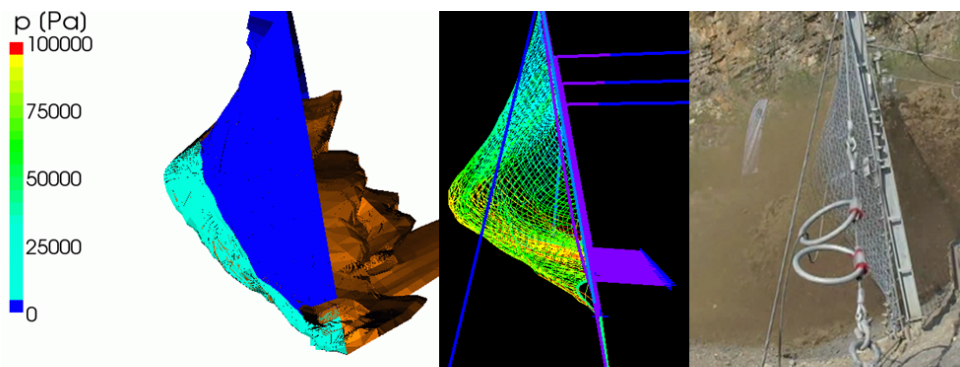


Figure 10: Full impact: The maximal impact wave reaches a height in OpenFOAM that is about the height witnessed at the experiment.

5 CONCLUSIONS

The development of flexible shallow landslide barriers is in need for numerical models. The state of the art to apply Finite-Element simulations for the design of the barrier structure was raised by developing a discrete element for the investigated net types that predicts not only the maximal load but the deformations with good accuracy. The loading of the barrier is conventionally simulated with static and equally distributed forces that do not account for the dynamic interaction. With the coupling of the structure code to a CFD simulation realized in OpenFOAM, the impact and the interaction between barrier and shallow landslide were successfully modelled, and should reduce the efforts needed in full scale prototype testing.

REFERENCES

- [1] Volkwein, A. *Numerische Simulation von flexiblen Steinschlagschutzsystemen*. Ph.D. Diss. Swiss Federal Inst. of Technology Zurich, Switzerland (2004).
- [2] Christen, M., Bartelt, P. and Gruber, U. *RAMMS - a Modelling System for Snow Avalanches, Debris Flows and Rockfalls based on IDL*. Photogramm. Fernerkund. Geoinf., (2007) **4**:289-292.
- [3] OpenFOAM: open source CFD, www.openfoam.com, visited 23.02.2011.
- [4] OpenFOAM LTT Rostock Extensions, www.ltt-rostock.de/mediawiki/index.php/LTTRostockExtensions, visited 23.02.2011.
- [5] Huhtanen, J. P. T. and Karvinen, R. J. *Interaction of Non-Newtonian Fluid Dynamics and Turbulence on the Behavior of Pulp Suspension Flows*. Annual transactions of the Nordic Rheology Society, (2005) **13**:177-186.

- [6] Jakob, M. and Hungr, O. *Debrisflow hazards and related phenomena*. Springer-Praxis Series in Geophysics, (2005) ISBN: 978-3-540-20726-9, p. 166-167.
- [7] Lei Wang and Xi-Yun Lu. *Large eddy simulation of stably stratified turbulent open channel flows with low- to high-Prandtl number*. International Journal of Heat and Mass Transfer (2005) **48**:1883-1897.
- [8] Hegglin, R., *Beiträge zum Prozessverständnis des fluvialen Geschiebetransports*. Master Thesis Institute of Geography, University of Bern, Switzerland (2010).
- [9] Kornev, N. V., Tkatchenko, I. V. and Hassel, E. H. *A simple clipping procedure for the dynamic mixed model based on Taylor series approximation*. Commun. Numer. Meth. Engng (2006) **22**:55-61.
- [10] Bugnion, L.; Volkwein, A., Wendeler, C. and Roth, A. *Large-scale field testing on flexible shallow landslide barriers*. Geophys. Res. Abstr. 12: EGU2010-11755 (2010).